plate. When the solution is cooled to -20 °C, a dark-green glass formed, and later yellow crystals. The yellow precipitate was collected, washed with cold ethanol, and then vacuum dried. The yield obtained was 1.6 g, mp 185-186 °C with bubbling (the crystals turned red at 160 °C).

2-Pyryldiazomethane. 2-Pyrenecarboxaldehyde *p*-toluenesulfonylhydrazone was treated with *n*-butyllithium according to the general procedure described. Infrared analysis of the product solid showed diazo absorption at 2070 cm^{-1}.

1-Naphthalene-α,α-dideuteriomethanol. Ten grams of 1-naphthoyl chloride in 200 mL of ether was added to 2.8 g of $LiAlD_4$ (Merck, >99.9%) in 150 mL ether. The addition was so regulated as to maintain a gentle reflux. The solution was stirred 12 h and then quenched with 2-propanol, then H_2O, then 150 mL of 30% aqueous KOH. The ether phase was separated, washed with water, dried over $MgSO_4$, and rotovapped to dryness. The residual oil crystallized on standing. It was recrystallized from ethanol–water to give 1.2 g of product, mp 62–63 °C. Mass spectral and proton NMR analysis showed >99% d_2.

1-Naphth-α-deuterioaldehyde. A 7-g sample of 1-naphthalene-α,α-dideuteriomethanol was added to a suspension of 30 g of MnO_2 in 500 mL of toluene which had been previously activated by azeotropic reflux for 12 h. The solution was filtered hot, and the solvent was removed, leaving 6.2 g of clear oil. NMR showed no aldehydic C-H. The infrared showed no C-H stretch at 2735 and 2840 but strong C–D at 2070 and 2120 cm^{-1}.

1-Naphth-α-deuterioaldehyde Hydrazone. A 1.1-g sample of 1-naphth-α-deuterioaldehyde was dissolved in 30 mL of absolute alcohol. To this was added 0.7 g of 97% hydrazine. The solution was concentrated to a volume of 7 mL by boiling on a hot plate. When the solution was cooled to -20 °C, the product precipitated. It was collected and air-dried, mp 83–88 °C. The mass spectrum showed >99% d_1. NMR analysis reveals that the H–C=N–N resonance at δ 8.3 had disappeared completely.

1-Naphthyl-α-deuteriodiazomethane. 1-Naphth-α-deuterioaldehyde hydrazone was oxidized with HgO according to the general procedure described. NMR analysis reveals that the H—C=N=N— resonance at δ 5.4 had disappeared completely.

Acknowledgment. We gratefully acknowledge support of this work by the National Science Foundation (Grant No. CH-7900896). The authors thank Professors Hine and McCurdy for valuable discussions.

Magnetic Studies and the Crystal and Molecular Structure of $[enH_2][V(hedta\text{-}H)]_2{\cdot}2H_2O$: A Novel Di-$\mu$-alcoxy-Bridged Dimer of Seven-Coordinate V(III)

Rex E. Shepherd,*[1a] William E. Hatfield,*[2] Debashis Ghosh,[1b] C. David Stout,[1b] Frank J. Kristine,[1a] and J. R. Ruble[1b]

Contribution from the Department of Chemistry and the Department of Crystallography, University of Pittsburgh, Pittsburgh, Pennsylvania 15260, and the Department of Chemistry, University of North Carolina at Chapel Hill, Chapel Hill, North Carolina 27514.

Received January 5, 1981. Revised Manuscript Received April 24, 1981

Abstract: The crystal and molecular structure of $[enH_2][V(hedta\text{-}H)]_2{\cdot}2H_2O$ has been determined from 2734 independent reflections (Mo Kα radiation) to $R = 0.042$ ($R_w = 0.035$). The structure displays novel bridging of the two V atoms by the alcoxy groups formed by deprotonation of the *N*-hydroxyethyl functionality of the parent hedta^{3-} ligand [hedta^{3-} = *N*-hydroxyethylethylenediaminetriacetate anion]. Each V(III) center in the dimer has sevenfold coordination which is approximated by a slightly distorted pentagonal bipyramid. The central angles of the alcoxy-bridged V_2O_2 core are virtually strain-free angles: V–O–V angles are 108°; O–V–O angles are 72°. The V–V separation is 3.296 Å. The magnetic susceptibilities of the $[enH_2][V(hedta\text{-}H)]_2{\cdot}2H_2O$ salt were determined from 4.24 to 91.4 K by the vibrating magnetometer method. The susceptibilities are consistent with a spin-only interaction of two d^2 centers described by the Hamiltonian, $-2J\mathbf{S}_1{\cdot}\mathbf{S}_2$. The best fit parameters for the susceptibility data are $g = 1.93$ and $-2J = 17.1$ cm^{-1}. The $2J$ value is consistent with the dialcoxy-bridging unit of the V_2O_2 core. The formation of the dialcoxy-bridged unit of the V(III) dimer in $[V(hedta\text{-}H)]_2{}^{2-}$ appears to account for the kinetically slow intramolecular electron-transfer reaction with $V^{II}OV^{IV}(hedta)_2{}^{2-}$.

Although the mechanistic aspects of the formation of the binuclear complex containing V(III) centers chelated by the hedta ligand have been studied,[3] it remained uncertain whether the V(III) centers are joined by an oxo ligand as in the Fe(III) complex, $[Fe(hedta)]_2O^{2-}$, or by dihydroxy-bridging ligands or by some other coordination arrangement. The binuclear complex, V(III, III), of this report is produced from monomeric V^{III}(hedta) by two paths: (1) by combination of two molecules of $V(hedta)(OH)^-$ or $V(hedta)(OH)^-$ and $V(hedta)(H_2O)^3$ or (2) by a novel redox reaction.[4,5] The cross reaction between $VO(hedta)^-$ and $V(hedta)^-$ produces the V(III, III) binuclear complex by two paths: (a) by intramolecular electron transfer within a $V^{II}V^{IV}O(hedta)_2{}^{2-}$ intermediate which is detectable on the stopped-flow time scale and (b) by combination of V(hedta) monomer species formed during the competitive outer-sphere electron-transfer path. On the basis of the solvent-exchange rate of V(II), the enhancement provided for solvent exchange with hedta^{3-} coordination on V(II), and the substitution-inert vanadyl oxygen in $VO(hedta)^-$, it has been concluded that the unusually intense spectral features of the $V^{II}V^{IV}O(hedta)_2{}^{2-}$ species, which differ from the less intense spectral parameters of the V(III, III) complex, originate in oxo bridging between V(II) and V(IV) in the cross reaction.[4,5] Although the V(II, IV) intermediate has a short lifetime of about 25 ms, this lifetime is actually unusually long

---

(1) (a) Department of Chemistry, University of Pittsburgh. (b) Department of Crystallography, University of Pittsburgh.

(2) Department of Chemistry, University of North Carolina at Chapel Hill.

(3) Kristine, F. J.; Shepherd, R. E. *J. Am. Chem. Soc.* **1977**, *99*, 6562.

(4) Kristine, F. J.; Shepherd, R. E. *J. Chem. Soc., Chem. Commun.* **1976**, 994.

(5) Kristine, F. J.; Shepherd, R. E. *J. Am. Chem. Soc.* **1978**, *100*, 4398.

0002-7863/81/1503-5511$01.25/0

in view of the absence of the detection of one-atom-bridged precursor complexes in other systems.[4,5] The intramolecular electron-transfer step has a substantially more negative ΔS_{ET}^{*} value than has been observed for other binuclear systems. Shepherd and Kristine concluded that structural rearrangement factors contribute to the activation entropy as a term, ΔS_{CR}^{*}, in addition to the usual inner-sphere bond length and solvation shell adjustments attributed to ΔS_{reorg}^{*} of the Marcus approach. Therefore any structural information that may establish the origin of the relatively slow intramolecular electron transfer for the $V^{II}V^{IV}O(hedta)_2^{2-}$ complex would be meaningful. The V(III, III) binuclear complex may be isolated as an ethylenediammonium salt.[3] Neither the infrared vibrational spectrum nor room-temperature magnetic susceptibilities could establish if an oxo-bridged or dihydroxy-bridged structure had obtained. The X-ray diffraction study in this report shows conclusively that neither of these units is present in the V(III, III) binuclear product. The proper formulation is $[enH_2][V(hedta\text{-}H)]_2\cdot 2H_2O$ where the $(hedta\text{-}H)^{4-}$ unit implies complete coordination of the three carboxylate donors, two ethylenediamine nitrogens, *and* the deprotonated alcoxy group of the parent $hedta^{3-}$ ligand. The proper structure at each V(III) center is a distorted pentagonal bipyramid as described here in detail. In concert with the structural determination, we have completed magnetic studies between 4 and 100 K which are consistent with the alcoxy-bridging units. The magnitude of the coupling of the two d^2 V(III) centers in the $[V(hedta\text{-}H)]_2^{2-}$ complex is comparable to dialcoxy- and dihydroxy-bridged transition-metal ions of the first series.

Experimental Section

1. X-ray Diffraction Data. The compound was prepared and crystallized as described by Kristine and Shepherd.[3] The crystals form as irregular prisms which were cut along the cleavage plane to obtain single rectangular crystals. The cell dimensions and space group were determined from a series of rotation, Weissenberg, and precession photographs. Two space groups are possible from systematic absences: *Pnma* (ϕkl absent for $k + l$ odd and $hk\phi$ absent for h odd) and $Pna2_1$ (b and c axes interchanged; ϕkl absent for $k + l$ odd and $h\phi l$ absent for h odd). For data collection the former was assumed.

The data were collected on the Department of Crystallography (Pittsburgh)[1b] CAD-4 diffractometer equipped with graphite monochromator. The wavelength used was Mo Kα (0.709 26 Å). A dark purple crystal of dimensions 0.5 × 0.4 × 0.15 mm^3 was chosen. All reflections were collected in the positive octant of the reflection sphere, between θ limits 2.0 and 25.0°. A ω scan was used for data collection and reflections for which $F_o \leq 1.56\sigma(F_o)$ were considered unobserved and flagged weak. The scan angle was 1.2°. With the use of these criteria, a data set of 2734 independent reflections was obtained. ψ scans revealed that absorption corrections were not necessary. A set of 40 high angle, randomly distributed strong reflections was chosen to obtain least-squares values of cell parameters.

During the data reduction, Lp corrections ($\theta_m = 6.1°$) were applied. Since the ψ scans were nearly flat, it was thought that correction for absorption was unnecessary. However, a theoretical calculation of absorption effects, following the identification of the crystal faces and measurement of distances between them, agreed very well with the experimental ψ scan.[6] A $N(Z^2)$ test following the Wilson plot suggested that the structure was noncentrosymmetric. Hence, the b and c axes were interchanged and l was changed to $-l$ to keep the axial system right handed.

A structure factor calculation with two V atoms using Wilson plot scale and temperature factors produced $R = 0.47$. A Fourier synthesis at this stage revealed 29 out of the remaining 44 nonhydrogen atoms. A second Fourier synthesis with 33 atoms yielded the rest of the atoms in the molecule and the solvents of crystallization.

Coordinates and thermal parameters of the 46 nonhydrogen atoms were refined by block-diagonal least-squares refinement, initially with isotropic temperature factors. After four cycles of refinement the R factor was 0.091. Another four cycles of refinement with anisotropic temperature factors brought the R value down to 0.056. All 42 hydrogens were located in a difference Fourier map at this stage. Electron densities at the hydrogen peaks ranged from 0.40 to 0.55 e$^-$/Å^3. All the hydrogens thus located were stereochemically reasonable. After four cycles of refinement with all 88 atoms (hydrogen temperature factors refined isotropically) and with correction for anomalous scattering by vanadium,[33] the refinement converged to $R = 0.042$ for 2734 reflections. The weighted R factor for observed reflections was 0.035. The weighing factor used was $1/\sigma(F_o^2)$, $\sigma(F_o)$'s being obtained from counting statistics. A final difference Fourier synthesis showed the highest peak of 0.402 e$^-$/Å^3 halfway between the line joining the vanadium atoms.

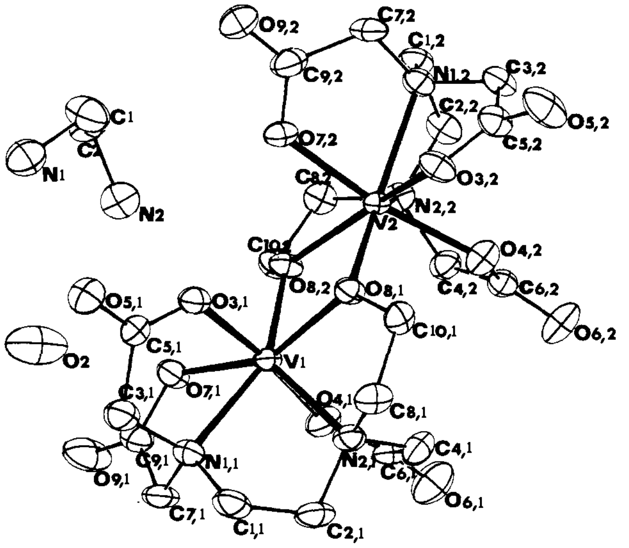

Figure 1. Nonhydrogen atom positions for the structure of $[enH_2]\cdot[V(hedta\text{-}H)]_2\cdot 2H_2O$ at $R = 0.042$.

2. Magnetic Studies. The magnetic susceptibilities for crystals of $[enH_2][V(hedta\text{-}H)]_2\cdot H_2O$ grown in the Department of Chemistry (Pittsburgh)[1a] laboratory were obtained between 4.24 and 91.9 K by using a Princeton Applied Research Model 155 vibrating sample magnetometer operated at a field strength of 10 000 G. Complete details of the procedure, including magnetic field and temperature calibrations, have been described.[7] Magnetic studies were carried out at the Department of Chemistry (North Carolina).[2]

3. Summary of Crystal Data: "molecular formula", $V_2O_{16}N_6C_{22}H_{42}$; space group, $Pna2_1$; $a = 19.579$ (5) Å, $b = 11.391$ (3) Å, $c = 13.399$ (2) Å; $Z = 4$; d(exptl) = 1.669 g/mL, d(calcd) = 1.665 g/mL; μ_{mass}(Mo Kα) = 4.54 cm^2/g, μ_{linear}(Mo Kα) = 7.58 cm^{-1}; $R = 0.042$, $R_w = 0.035$.

Results and Discussion

Structure of $[enH_2][V(hedta\text{-}H)]_2\cdot 2H_2O$. The structure of $[enH_2][V(hedta\text{-}H)]_2\cdot 2H_2O$ as determined by the methods described in the Experimental Section is shown in Figure 1 for all nuclei except hydrogen nuclei which are omitted for clarity. The atoms of the central coordination about the V(III) centers are shown in Figure 2. Hydrogen-bonding interactions between the enH_2^{2+} cation and H_2O molecules of the lattice are shown in Figure 3. The unit cell ($Z = 4$) is shown in Figure 4. Positional parameters for nonhydrogen atoms are given in Tables Ia,b available as supplementary material. Structural factors are available in Tables SI, SII, and SIII in microfilm.

The structure of $[enH_2][V(hedta\text{-}H)]_2\cdot 2H_2O$ is unusual with respect to analogous metal ion $edta^{4-}$ or $hedta^{3-}$ complexes. Reports of other seven-coordinate V(III) complexes appear to be limited to $V(CN)_7^{4-}$ produced under forcing conditions with 3 M KCN. The structure of $K_4V(CN)_7\cdot 2H_2O$ is a slightly distorted pentagonal bipyramid of approximately D_{5h} symmetry.[8] The structure of $[enH_2][V(hedta\text{-}H)]_2\cdot 2H_2O$ differs from the known structures of the edta family of transition-metal complexes in the following regards.

(i) The bridging oxygens are the alcoxy oxygens, one each from the $(hedta\text{-}H)^{4-}$ ligands. In other coordination complexes of transition metals the bridging oxygen is either an oxo ligand or hydroxyl or alcoxy groups from the solvent.

(ii) Each vanadium is coordinated by seven atoms, two nitrogen and five oxygens. These seven atoms are distributed in two planes, a four-atom plane and a nearly parallel three-atom plane, on the

---

(6) Busing, W. R.; Levy, H. A. *Acta Crystallogr.* **1957**, *10*, 180.

(7) Losee, D. B.; Hatfield, W. E. *Phys. Rev. B* **1974**, *10*, 212.

(8) Levenson, R. A.; Towns, R. L. *Inorg. Chem.* **1974**, *13*, 105.

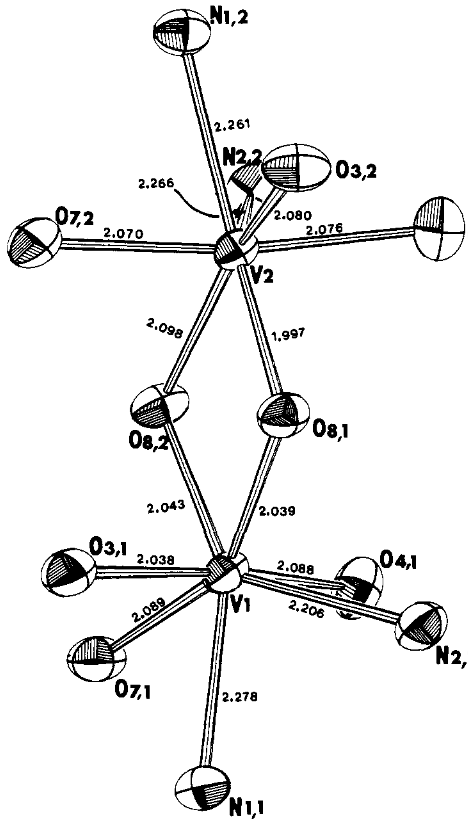

Figure 2. Bond distances and atom locations of first coordination sphere of V(III) centers in [enH$_2$][V(hedta-H)]$_2$·2H$_2$O.

other side of the vanadium center. The four-atom planes are formed by two ethylenediamine backbone nitrogens, one alcoxy-bridging oxygen, and a carboxylate oxygen ($N_{1,1}$, $N_{2,1}$, $O_{3,1}$, and $O_{8,1}$ for V_1 and $N_{1,2}$, $N_{2,2}$, $O_{7,2}$, and $O_{8,2}$ for V_2) (see Table SII) for least-squares planes). Deviations from the least-squares planes are less than 0.2 Å in all cases. The three-atom planes through $O_{8,2}$, $O_{4,1}$, and $O_{7,1}$ for V_1 and $O_{3,2}$, $O_{4,2}$, and $O_{8,1}$ for V_2 are nearly parallel to the four-atom planes. The four-atom plane and three-atom plane deviate from strict parallel geometry by 3.95° for V_1 and 1.05° for V_2. The two sets of planes are tilted to each other by an average angle of 45.38° (see Table SII of the supplementary material). It remains more useful to consider the coordination at each V(III) site as a distorted pentagonal bipyramid with axial carboxylate donors; this structural feature will be discussed more fully in the comparison of the [V(hedta-H)]$_2^{2-}$ unit with other metal ion edta and hedta complexes.

The bond distances and angles for nonhydrogen bonded atoms are listed respectively in a and b of Table I. Bond distances involving hydrogen are listed in Table Ic. The bond distances and angles reveal that the coordination at each V(III) site is essentially similar, except for a few differences. The V_1–$N_{2,1}$ distance (2.21 Å) is shorter than the other three V–N distances (~2.27 Å). The V_1–$O_{3,1}$ distance (2.04 Å) is slightly shorter than the average distance to the other carboxylates (average ~2.08 Å).

Some asymmetry in the structure between the two halves of the bridged dimer is apparently introduced by the intra- and intermolecular hydrogen bonds which the molecule makes with the enH$_2^{2+}$ unit and with the two solvent molecules in the lattice. These hydrogen-bonding contributions may prevent the molecule from being crystallized in a centrosymmetric space group (see Table Ic). One of the bridging alcoxy oxygens ($O_{8,2}$) makes a hydrogen bond with the ethylenediammonium cation (N_2–H_2···$O_{8,2}$) while the other alcoxy oxygen ($O_{8,1}$) does not. This is consistent with the fact that V_1–$O_{8,2}$ and V_2–$O_{8,2}$ bond distances are longer than V_1–$O_{8,1}$ and V_2–$O_{8,1}$ distances (see Table IIa). Again, $O_{9,1}$ makes hydrogen bonds with both water molecules but $O_{9,2}$ does not. This is also consistent with slightly longer $C_{9,1}$–$O_{9,1}$ than the corresponding distance in the other half. Two intermolecular hydrogen bonds formed by ethylenediamine nitrogens (N_2–H_1···$O_{6,2}$ and N_1–H_3···O_1) are fairly short. These strong

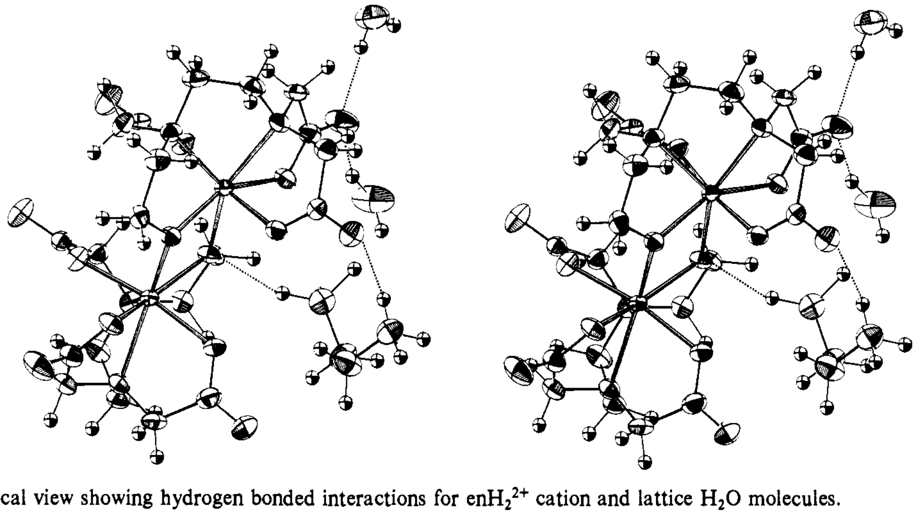

Figure 3. Stereochemical view showing hydrogen bonded interactions for enH$_2^{2+}$ cation and lattice H$_2$O molecules.

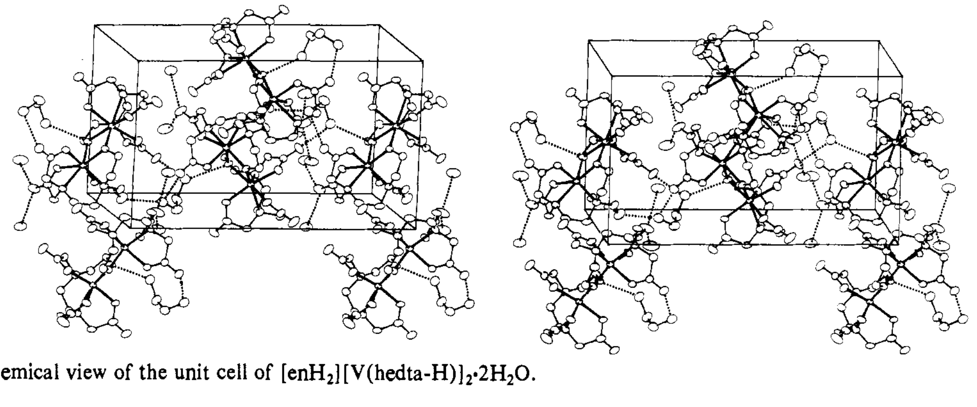

Figure 4. Stereochemical view of the unit cell of [enH$_2$][V(hedta-H)]$_2$·2H$_2$O.

Table I

(a) Bond Distances (Å) Involving Nonhydrogen Atoms

$N_{1,1}-V_1$	2.278 (4)	$C_{5,1}-O_{3,1}$	1.268 (6)
$N_{1,1}-C_{1,1}$	1.474 (7)	$C_{5,1}-O_{5,1}$	1.238 (6)
$N_{1,1}-C_{3,1}$	1.483 (7)	$C_{9,1}-O_{7,1}$	1.271 (7)
$N_{1,1}-C_{7,1}$	1.470 (7)	$C_{9,1}-O_{9,1}$	1.237 (7)
$N_{2,1}-V_1$	2.206 (4)	$C_{6,1}-O_{4,1}$	1.282 (6)
$N_{2,1}-C_{2,1}$	1.484 (7)	$C_{6,1}-O_{6,1}$	1.220 (7)
$N_{2,1}-C_{4,1}$	1.482 (7)	$C_{10,}-O_{8,1}$	1.424 (6)
$N_{2,1}-C_{8,1}$	1.478 (7)	$O_{3,1}-V_1$	2.038 (4)
$C_{1,1}-C_{2,1}$	1.507 (8)	$O_{7,1}-V_1$	2.089 (4)
$C_{3,1}-C_{5,1}$	1.504 (8)	$O_{4,1}-V_1$	2.088 (4)
$C_{7,1}-C_{9,1}$	1.517 (8)	$O_{8,1}-V_1$	2.039 (3)
$C_{4,1}-C_{6,1}$	1.534 (8)	$O_{8,2}-V_1$	2.043 (3)
$C_{8,1}-C_{10,1}$	1.505 (8)		
$N_{1,2}-V_2$	2.261 (4)	$C_{5,2}-O_{3,2}$	1.268 (7)
$N_{1,2}-C_{1,2}$	1.476 (7)	$C_{5,2}-O_{5,2}$	1.236 (7)
$N_{1,2}-C_{3,2}$	1.492 (7)	$C_{9,2}-O_{7,2}$	1.288 (7)
$N_{1,2}-C_{7,2}$	1.476 (7)	$C_{9,2}-O_{9,2}$	1.218 (8)
$N_{2,2}-V_2$	2.266 (4)	$C_{6,2}-O_{4,2}$	1.277 (6)
$N_{2,2}-C_{2,2}$	1.485 (7)	$C_{6,2}-O_{6,2}$	1.242 (6)
$N_{2,2}-C_{4,2}$	1.475 (7)	$C_{10,2}-O_{8,2}$	1.418 (6)
$N_{2,2}-C_{8,2}$	1.483 (7)	$O_{3,2}-V_2$	2.080 (4)
$C_{1,2}-C_{2,2}$	1.512 (8)	$O_{7,2}-V_2$	2.070 (4)
$C_{3,2}-C_{5,2}$	1.518 (8)	$O_{4,2}-V_2$	2.076 (3)
$C_{7,2}-C_{9,2}$	1.507 (8)	$O_{8,2}-V_2$	2.098 (3)
$C_{4,2}-C_{6,2}$	1.510 (7)	$O_{8,1}-V_2$	1.997 (3)
$C_{8,2}-C_{10,2}$	1.492 (7)		
N_1-C_1	1.458 (8)	$V_1\cdots V_2$	3.296 (1)
N_2-C_2	1.483 (8)	$O_{8,1}\cdots O_{8,2}$	2.396 (5)
C_1-C_2	1.495 (9)		

(b) Bond Angles (Deg) Involving Nonhydrogen Atoms

$C_{1,1}-N_{1,1}-C_{3,1}$	111.4 (4)	$N_{2,1}-C_{4,1}-C_{6,1}$	109.5 (4)
$C_{1,1}-N_{1,1}-C_{7,1}$	110.7 (4)	$N_{2,1}-C_{8,1}-C_{10,1}$	108.7 (4)
$C_{3,1}-N_{1,1}-C_{7,1}$	109.2 (4)	$C_{3,1}-C_{5,1}-O_{3,1}$	116.9 (5)
$C_{1,1}-N_{1,1}-V_1$	112.2 (3)	$C_{3,1}-C_{5,1}-O_{5,1}$	117.7 (5)
$C_{3,1}-N_{1,1}-V_1$	108.6 (3)	$O_{3,1}-C_{5,1}-O_{5,1}$	125.3 (5)
$C_{7,1}-N_{1,1}-V_1$	104.5 (3)	$C_{7,1}-C_{9,1}-O_{7,1}$	115.6 (5)
$C_{2,1}-N_{2,1}-C_{4,1}$	108.4 (4)	$C_{7,1}-C_{9,1}-O_{9,1}$	120.5 (5)
$C_{2,1}-N_{2,1}-C_{8,1}$	111.2 (4)	$O_{7,1}-C_{9,1}-O_{9,1}$	123.9 (5)
$C_{4,1}-N_{2,1}-C_{8,1}$	110.6 (4)	$C_{4,1}-C_{6,1}-O_{4,1}$	113.9 (4)
$C_{2,1}-N_{2,1}-V_1$	113.0 (3)	$C_{4,1}-C_{6,1}-O_{6,1}$	119.8 (5)
$C_{4,1}-N_{2,1}-V_1$	107.0 (3)	$O_{4,1}-C_{6,1}-O_{6,1}$	126.2 (5)
$C_{8,1}-N_{2,1}-V_1$	106.5 (3)	$C_{8,1}-C_{10,1}-O_{8,1}$	107.5 (4)
$N_{1,1}-C_{1,1}-C_{2,1}$	109.7 (5)	$C_{5,1}-O_{3,1}-V_1$	123.3 (3)
$C_{1,1}-C_{2,1}-N_{2,1}$	108.7 (5)	$C_{9,1}-O_{7,1}-V_1$	119.8 (3)
$N_{1,1}-C_{3,1}-C_{5,1}$	112.8 (5)	$C_{6,1}-O_{4,1}-V_1$	120.5 (3)
$N_{1,1}-C_{7,1}-C_{9,1}$	107.7 (4)	$C_{10,1}-O_{8,1}-V_1$	122.3 (3)
$N_{1,1}-V_1-N_{2,1}$	75.6 (2)	$O_{7,1}-V_1-N_{2,1}$	135.1 (2)
$N_{1,1}-V_1-O_{3,1}$	76.3 (1)	$O_{7,1}-V_1-O_{4,1}$	80.7 (1)
$N_{1,1}-V_1-O_{7,1}$	72.7 (1)	$O_{7,1}-V_1-O_{8,1}$	150.5 (1)
$N_{1,1}-V_1-O_{4,1}$	100.6 (1)	$O_{7,1}-V_1-O_{8,2}$	81.2 (1)
$N_{1,1}-V_1-O_{8,1}$	129.9 (1)	$O_{4,1}-V_1-N_{2,1}$	74.7 (2)
$N_{1,1}-V_1-O_{8,2}$	151.7 (1)	$O_{4,1}-V_1-O_{8,1}$	108.5 (1)

(b) Bond Angles (Deg) Involving Nonhydrogen Atoms

$O_{3,1}-V_1-N_{2,1}$	115.0 (2)	$O_{4,1}-V_1-O_{8,2}$	85.4 (1)
$O_{3,1}-V_1-O_{7,1}$	87.4 (1)	$O_{8,1}-V_1-N_{2,1}$	74.1 (1)
$O_{3,1}-V_1-O_{4,1}$	168.0 (1)	$O_{8,1}-V_1-O_{8,2}$	71.9 (1)
$O_{3,1}-V_1-O_{8,1}$	81.7 (1)	$O_{8,2}-V_1-N_{2,1}$	132.2 (1)
$O_{3,1}-V_1-O_{8,2}$	92.1 (1)		
$C_{1,2}-N_{1,2}-C_{3,2}$	113.3 (4)	$N_{2,2}-C_{4,2}-C_{6,2}$	109.8 (4)
$C_{1,2}-N_{1,2}-C_{7,2}$	109.7 (4)	$N_{2,2}-C_{8,2}-C_{10,2}$	108.0 (4)
$C_{3,2}-N_{1,2}-C_{7,2}$	108.7 (4)	$C_{3,2}-C_{5,2}-O_{3,2}$	114.8 (4)
$C_{1,2}-N_{1,2}-V_2$	112.3 (3)	$C_{3,2}-C_{5,2}-O_{5,2}$	119.4 (5)
$C_{3,2}-N_{1,2}-V_2$	104.0 (3)	$O_{3,2}-C_{5,2}-O_{5,2}$	125.7 (5)
$C_{7,2}-N_{1,2}-V_2$	108.6 (3)	$C_{7,2}-C_{9,2}-O_{7,2}$	116.0 (5)
$C_{2,2}-N_{2,2}-C_{4,2}$	107.8 (4)	$C_{7,2}-C_{9,2}-O_{9,2}$	118.7 (5)
$C_{2,2}-N_{2,2}-C_{8,2}$	111.5 (4)	$O_{7,2}-C_{9,2}-O_{9,2}$	125.2 (5)
$C_{4,2}-N_{2,2}-C_{8,2}$	111.5 (4)	$C_{4,2}-C_{6,2}-O_{4,2}$	114.6 (4)
$C_{2,2}-N_{2,2}-V_2$	111.8 (3)	$C_{4,2}-C_{6,2}-O_{6,2}$	120.0 (5)
$C_{4,2}-N_{2,2}-V_2$	107.2 (3)	$O_{4,2}-C_{6,2}-O_{6,2}$	125.4 (5)
$C_{8,2}-N_{2,2}-V_2$	106.9 (3)	$C_{8,2}-C_{10,2}-O_{8,2}$	108.3 (4)
$N_{1,2}-C_{1,2}-C_{2,2}$	108.7 (4)	$C_{5,2}-O_{3,2}-V_2$	119.4 (3)
$C_{1,2}-C_{2,2}-N_{2,2}$	109.4 (4)	$C_{9,2}-O_{7,2}-V_2$	121.3 (3)
$N_{1,2}-C_{3,2}-C_{5,2}$	106.6 (4)	$C_{6,2}-O_{4,2}-V_2$	122.6 (3)
$N_{1,2}-C_{7,2}-C_{9,2}$	111.4 (4)	$C_{10,2}-O_{8,2}-V_2$	122.0 (3)
$N_{1,2}-V_2-N_{2,2}$	75.5 (2)	$O_{7,2}-V_2-N_{2,2}$	106.7 (1)
$N_{1,2}-V_2-O_{3,2}$	71.5 (1)	$O_{7,2}-V_2-O_{4,2}$	171.5 (1)
$N_{1,2}-V_2-O_{7,2}$	74.7 (1)	$O_{7,2}-V_2-O_{8,2}$	78.8 (1)
$N_{1,2}-V_2-O_{4,2}$	97.4 (1)	$O_{7,2}-V_2-O_{8,1}$	98.8 (1)
$N_{1,2}-V_2-O_{8,2}$	130.3 (1)	$O_{4,2}-V_2-N_{2,2}$	73.6 (1)
$N_{1,2}-V_2-O_{8,1}$	152.7 (1)	$O_{4,2}-V_2-O_{8,2}$	109.1 (1)
$O_{3,2}-V_2-N_{2,2}$	134.9 (1)	$O_{4,2}-V_2-O_{8,1}$	86.9 (1)
$O_{3,2}-V_2-O_{7,2}$	93.5 (1)	$O_{8,2}-V_2-N_{2,2}$	73.0 (1)
$O_{3,2}-V_2-O_{4,2}$	81.0 (1)	$O_{8,2}-V_2-O_{8,1}$	72.0 (1)
$O_{3,2}-V_2-O_{8,2}$	151.8 (1)	$O_{8,1}-V_2-N_{2,2}$	131.0 (1)
$O_{3,2}-V_2-O_{8,1}$	82.7 (1)		
$N_1-C_1-C_2$	114.0 (5)	$C_1-C_2-N_2$	112.0 (5)

(c) Hydrogen Bond Distances (Å) and Angles (Deg)[a]

acceptor symm	translatn	D-H···A	dist H···A	angle D-H-A	dist D-A
x, y, z	555	$O_1-H_2\cdots O_{9,1}$	1.74 (5)	154 (5)	2.660 (7)
x, y, z	555	$O_2-H_2\cdots O_{9,1}$	1.92 (5)	160 (5)	2.774 (6)
x, y, z	555	$N_1-H_2\cdots O_{5,1}$	2.00 (6)	155 (6)	2.781 (6)
x, y, z	555	$N_2-H_2\cdots O_{8,2}$	2.11 (5)	149 (4)	3.072 (6)
$^1/_2 + x, {}^1/_2 - y, z$	555	$N_1-H_1\cdots O_{6,1}$	1.88 (6)	164 (5)	2.859 (7)
$^1/_2 + x, {}^1/_2 - y, z$	555	$N_2-H_1\cdots O_{6,2}$	1.66 (6)	171 (5)	2.819 (6)
$^1/_2 - x, {}^1/_2 + y, {}^1/_2 + z$	444	$N_1-H_3\cdots O_1$	1.42 (8)	172 (7)	2.662 (7)
$^1/_2 - x, {}^1/_2 + y, {}^1/_2 + z$	455	$O_2-H_1\cdots O_{5,1}$	1.78 (4)	168 (4)	2.749 (6)

[a] Donor symmetry: x, y, z.

Table II. Deviations (Å) of Atoms from an Idealized Five-Coordinate Plane about V(III) Centers

plane 1			plane 2		
atom	dev	std dev	atom	dev	std dev
V_1	0.004 36	0.000 68	V_2	0.014 37	0.000 76
$N_{1,1}$	0.492 59	0.004 30	$N_{1,2}$	0.480 34	0.004 04
$N_{2,1}$	−0.654 31	0.004 26	$N_{2,2}$	−0.637 36	0.004 07
$O_{7,1}$	−0.165 90	0.003 54	$O_{3,2}$	−0.195 25	0.003 49
$O_{8,1}$	0.541 63	0.003 25	$O_{8,1}$	−0.203 79	0.003 15
$O_{8,2}$	−0.167 66	0.003 24	$O_{8,2}$	0.541 71	0.003 22

hydrogen bonds may be a consequence of the fact that the amines are protonated. It is also to be noted that these hydrogen bond angles are close to 180° (Table Ic). This fact is reaffirmed by unusually long N–H distances in ethylenediamine molecule. Again, $O_{5,1}$ makes hydrogen bonds ($N_1-H_2\cdots O_{5,1}$ and $O_2-H_1\cdots O_{5,1}$) but the corresponding oxygen in the other half of the molecule does not.

Apparently, the proximity of solvent molecules to half of the binuclear core seems to govern the structural differences between the two halves of the bridged dimer.

Comparison with Other Structures. The seven-coordinate structure for $[enH_2][V(hedta\text{-}H)]_2\cdot 2H_2O$ is shown in Figure 1. An idealized seven-coordinate structure having two axial ligands and five in-plane ligands should have the axial ligands at 180.0° and the in-plane L–M–L angles of 72.0°. The structure found for the $[V(hedta\text{-}H)]_2^{2-}$ unit approximates this structure reasonably well, with moderate distortions. The axial angles $O_{3,1}-V_1-O_{4,1}$ and $O_{7,2}-V_2-O_{4,2}$ are 168.0 and 171.5° while the angle sums in the approximate plane about V_1 and V_2 are 375.5 and 374.5°, respectively. The sum of in-plane angles exceeds 360.0° by ca. 15° which causes slight ruffling in the positions of the "in-plane" O and N donors. The deviation from ideal angles of 72.0° presumably occurs to accommodate the formation of the five-member chelate rings of the $(hedta\text{-}H)^{4-}$ ligand. The largest "in-plane" angle occurs between the coordinated in-plane carboxylate ligand and the bridging alcoxy oxygen provided by the

Table III. X-ray Diffraction Data for Some M^{III}edta Family Complexes

(A) Bond Distances (Å) to First Coordination Sphere

M(III) complex (ref)	coord no.	M-N	$M\text{-}(CO_2^-)$	$d_{M-O(bridge)}$, Å
$[V(hedta\text{-}H)]_2^{2-}$ (this work)	7	2.27 2.24	2.075	2.07 2.02
$[Cr(edda)(OH)]_2$ (10)	6	2.09 2.07	1.981	1.964
$[Mn(edta)^-]$ (9)	6	2.21	1.90 2.02	
$[Fe(hedta)_2O]^{2-}$ (11)	6	2.27 2.20	2.03	1.79
$[Fe(edtaH)(H_2O)]$ (12)	6	2.22	2.00	
$[Fe(edta)(H_2O)^-]$ (12)	7	2.33	2.057	
$[Co(edta)^-]$ (13)	6	1.93	1.91	

(B) Bridging Angles (Deg) in Binuclear Complexes

M(III) complex (ref)	M–O–M	d_{M-M}, Å
$[(Fe(hedta))_2O]^{2-}$ (11)	165.0	3.549
$[V(hedta\text{-}H)]_2^{2-}$ (this work)	108	3.296
$[Cr(edda)(OH)_2$ (10)	97.6	2.950

$(hedta\text{-}H)^{4-}$ ligand of the opposite V(III) center. These angles are 81.2 and 82.7°; the other in-plane angles are a maximum of 3.6° larger than 72° with the $O_{8,2}$–V_1–$O_{8,1}$ and $O_{8,2}$–V_2–$O_{8,1}$ core angles 71.9 and 72.0°. The idealized seven-coordinate structure is therefore a useful view of the coordination at each V(III) center. The data in Table II show the deviations of atoms in the idealized five-coordinate plane about each V(III) center. Ruffling of the "in-plane" O and N donors is shown by reasonably large deviations of ca. 0.5–0.6 Å for the ethylenediamine nitrogens and one alcoxy-bridging oxygen at each V(III) center. Least-squares planes calculated for ligand donor atoms only (a five-atom fit) passed through the coordinates of each V(III) center. Deviation from linearity of the axial ligands is observed even for the six-coordinate complexes; for example the axial O–Mn–O angle in $Mn(edta)^-$ is 173.8°.[9] Bond distance and angular data for $[enH_2][V(hedta\text{-}H)]_2\cdot 2H_2O$ may be compared to the related binuclear complexes $[Cr(edda)(OH)]_2$[10] and $[enH_2][(Fe(hedta))_2O]\cdot 6H_2O$.[11] The monomeric complexes $K[Mn(edta)]\cdot 2H_2O$, $Fe(edtaH)(H_2O)$,[12] $Fe(edta)(H_2O)^-$,[12] and $[NH_4][Co(edta)]\cdot 2H_2O$[13] are also informative in establishing structural characteristics normally observed for M^{III}edta family complexes of the first transition series. Bond distances and angle parameters for these complexes have been collected in Table III. The values given for ionic radii of the M(III) ions of the first transition series are very similar: V(III), 0.78 Å; Cr(III), 0.76 Å; Mn(III), 0.72 Å; Fe(III), 0.79 Å; Co(III), 0.68 Å.[31] The similar size of these ions suggests that factors other than ionic size will dominate the bonding to edta-like ligands in the first transition series.

M–N Distance. The V–N distances (average V–N = 2.25 Å) in the $[V(hedta\text{-}H)]_2^{2-}$ unit are longer than those found in $[VCl_3(N(CH_3)_3)_2]$ (2.195, 2.230 Å).[14] It would be anticipated that V–N bonds in the seven-coordinate $[V(hedta\text{-}H)]_2^{2-}$ species would be longer than in the five-coordinate $VCl_3(N(CH_3)_3)_2$ complex. The structures of the six-coordinate $Fe(edtaH)(H_2O)$ and seven-coordinate $Fe(edta)(H_2O)^-$ species show that the bond distances of the first coordination sphere atoms to the Fe(III) center are shorter in coordination number six than in seven.[12] The Fe–N distance is shorter by 0.10 Å while the Fe–O distance is shorter by ca. 0.06 Å in six-coordination with the edta environment. The M–N distance is anticipated to decrease in a steady manner as the effective nuclear charge, Z^*, increases across the transition series. Values suitable for comparison of the M–N distances in coordination number six may be obtained by subtracting 0.10 Å from the M–N distance of complexes in coordination number seven. The values for the M–N distance in six-coordination may be called d'_{M-N} to include both data sets for the measured and corrected six-coordination M–N distances. The values for d'_{M-N} and Z^*, evaluated by Slater's rules, are found as follows (M, d'_{M-N}, Z^*): V, 2.16 Å, 4.65; Cr, 2.09 Å, 5.30; Mn, 2.21 Å, 5.95; Fe, 2.22 Å, 6.60; Co, 1.93 Å, 7.25. It is reasonable to anticipate an expansion for the Mn(III) and Fe(III) high-spin complexes since these have, respectively, one and two electrons in orbitals of antibonding character (d_{z^2}, $d_{x^2-y^2}$). The V(III), Cr(III), and Co(III) complexes have electrons populating orbitals which point away from bond axes. These complexes exhibit a correlation between d'_{M-N} and Z^* for these ions as in eq 1. The deviation

$$d'_{M-N} = (2.58 \pm 0.03) - (8.14 \pm 0.46) \times 10^{-2} Z^* \quad (1)$$

in d'_{M-N} for Mn(III) and Fe(III) as evaluated from eq 1 is +0.11 and +0.18 Å. These deviations correspond to the expansion of the M–N distance by ca. 0.10 Å per antibonding electron.

M–O Distances. The carboxylic acid donor oxygens $O_{3,1}$, $O_{7,1}$, and $O_{4,1}$ for V_1 and $O_{3,2}$, $O_{4,2}$, and $O_{7,2}$ for V_2 are an average of 2.074 Å from the respective V(III) center. The bridging oxygen $O_{8,1}$ has an average V–O distance of 2.02 Å while the second alcoxy-bridging oxygen ($O_{8,2}$) which is hydrogen bonded to the ethylenediammonium cation exhibits slightly longer V–O bonds (average d_{V-O} = 2.04 Å). The V–O distance in $V(acac)_3$ is 1.979 Å.[15] The shortened distance from 2.09 Å has been taken to imply a greater multiple bond character in the V–O bond of $V(acac)_3$ than the Fe–O bond of $Fe(acac)_3$.[15] In $Fe(acac)_3$ the Fe–O distance equals the sum of the ionic radii. The V–O distances found in $[V(hedta\text{-}H)]_2^{2-}$ suggest that the carboxylate oxygen–V(III) bond is predominantly ionic while the shorter V–alcoxy oxygen bonds contain some covalent contribution in the bridging V–O bonds. The multiple bond character is less than for $V(acac)_3$, however.

The largest M–M separation of the binuclear ions in Table III is found for the oxo-bridged $[(Fe(hedta))_2O]^{2-}$ species. The Fe–O–Fe unit deviates from linearity by 15° (∠Fe–O–Fe = 165°). The oxo bridge provides a pathway for strong antiferromagnetic coupling (cf. Table V), and the Fe–O bridge distance is a short 1.79 Å, compared to the Fe–O carboxylic acid distance of 2.03 Å. With two bridging groups in $[V(hedta\text{-}H)]_2^{2-}$ the V–V distance is shorter than the $[(Fe(hedta))_2O]^{2-}$ unit (3.296 Å vs. 3.549 Å). The ∠V–O–V is 108°, almost unperturbed from the sp^3 angle of 109.5°. As discussed above, the ∠O–V–O is 72° in virtual agreement with anticipated angle of five groups coordinated around the girdle of V(III) with two axial groups to complete seven-coordination. *The central angles of the V_2O_2 core unit appear to have minimum strain consistent with seven-coordination and alcoxy-bridging oxygen donors.* By contrast the Cr_2O_2 core of $[Cr(edda)(OH)]_2$ has Cr–O–Cr angles of 97.6° and O–Cr–O angles of 82.4°.[10] The O–Cr–O angle is close to the 90.0° value of ideal octahedral coordination; however, the bridging Cr–O–Cr angle is the smallest of the Cr(III) dimeric complexes, yielding the shortest Cr–Cr distance of 2.950 Å.[10] The magnetic interaction of the Cr(III) centers in $[Cr(edda)(OH)]_2$ is the subject of a separate report.[16]

Because the metal ion radii are all approximately 0.78 Å for V(III), Cr(III), and Fe(III), the longest M–M distance for the oxo-bridged complex of Fe(III) followed by the $[V(hedta\text{-}H]_2^{2-}$ species and then by $[Cr(edda)(OH)]_2$ reveals that the $[V(hedta)]_2^{2-}$ system represents an intermediate case between M–O–M complexes in which the bridging angle approaches linearity (165°)

---

[9] Stein, J.; Fackler, J. P.; McClune, G. J.; Fee, J. A.; Chan, L. T. *Inorg. Chem.* **1979**, *18*, 3511.

[10] Srdanov, G.; Herak, R.; Radanović, D. J.; Veselinović, D. S. *Inorg. Chim. Acta* **1980**, *38*, 37.

[11] Lippard, S. J.; Schugar, H. J.; Walling, C. *Inorg. Chem.* **1967**, *6*, 1825.

[12] (a) Hoard, J. L.; Kennard, C. H. L.; Smith, G. S. *Inorg. Chem.* **1963**, *2*, 1316. (b) Hamor, M. J.; Hamor, T. A.; Hoard, J. L. *Ibid.* **1964**, *3*, 34.

[13] Weakliem, H. A.; Hoard, J. L. *J. Am. Chem. Soc.* **1959**, *81*, 549.

[14] Greene, P. T.; Orioli, P. L. *J. Chem. Soc. A* **1969**, 1621.

[15] Morosin, B.; Montgomery, H. *Acta Cryst (B)*, **1969**, *B25*, 1354.

[16] Hatfield, W. E.; MacDougall, J. J.; Shepherd, R. E., accepted for publication in *Inorg. Chem.*

for $[Fe(hedta)_2]_2O^{2-}]$ and the strained angle of 97.6° in $[Cr(edda)(OH)]_2$ where the dihydroxy bridge unit obtains with retention of a six-coordinate metal center. In the case of the V(III) system the dialcoxy structure is made more striking in that the binuclear ion may be synthesized by two independent routes. One path involved the hydrolytic dimerization of $V(hedta)(H_2O)$ which is presumably six-coordinate in solution with a pendant $-CH_2CH_2OH$ functionality.[3] The second path for production of $[V(hedta\text{-}H)]_2^{2-}$ occurs via the intramolecular electron-transfer pathway in the cross reaction of $VO(hedta)^-$ and $V(hedta)(H_2O)^-$.[4,5] Again both reactant species are other than seven-coordinate. $VO(hedta)^-$ is five-coordinate with only weak axial association trans to V=O with the solvent. The $V(hedta)(H_2O)^-$ complex is presumably six-coordinate with a pendant $-CH_2CH_2OH$. An intermediate in the cross reaction is observed, and this species is believed to be the mixed oxidation state binuclear complex, $(hedta)V^{III}OV^{IV}(hedta)^{2-}$,[4,5] in which the vanadium centers are bridged by the oxo ligand introduced by $VO(hedta)^-$. The electron-transfer process produces the dialcoxy bridge species $[V(hedta\text{-}H)]_2^{2-}$ by a process which is quite slow for metal centers bridged by a single O atom. The activation entropy is significantly negative as would be expected for the large reorganization in changing the coordination number at both vanadium centers ($\Delta S^{\ddagger} = -25$ eu).[5] What remains surprising is that the dialcoxy-bridged structure of seven-coordination is more favored over a six-coordinate structural analogue of $[Fe(hedta)]_2O^{2-}$ even when the V–O–V core is already assembled. The limiting steps in the redox transformation (rds) then would appear to be the conversion of the oxo-bridged core into the dialcoxy-bridged core, eq 2, with the extrusion of H_2O. Part of the driving force for the reorganization process must involve the gain in entropy for the release of a water molecule (ca. +15 eu) and, perhaps, water molecules hydrogen bonded to the pendant alcohol and carboxylate moieties of the reactant to compensate for the structural ordering in the product.

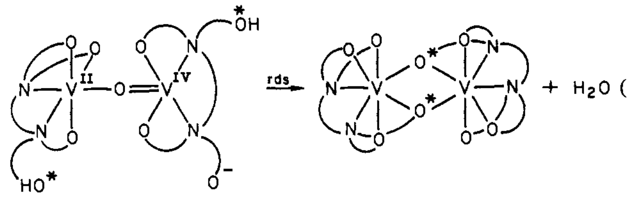

(2)

Ring Strain in $[V(hedta\text{-}H)]_2^{2-}$. Weakliem and Hoard proposed that the sum of angles of the five-member chelate rings could be used as a measure of the strain in forming the chelate–metal ion bond.[13] Within the edta family of chelates the ethylenediamine backbone (E ring) should form an idealized structure with a sum of the ring angles equal to 527.9° while the glycinate rings with no strain would have an angle sum of 538.9°. In the hexadentate complexes of edta such as $Co(edta)^-$ and $Mn(edta)^-$ two types of the glycinato rings are observed. The less strained out-of-plane rings have been designated R rings while those in the bonding plane of the ethylenediamine nitrogens are designed G rings. In order to compare the seven-coordinate V(III) centers in the $[V(hedta\text{-}H)]_2^{2-}$ species to $Co(edta)^-$ and the binuclear $[Cr(edda)(OH)]_2$, we have adopted the similar notation that the chelate rings including pseudoaxial bonded carboxylates will be designated R rings. Those carboxylate groups in the approximate equatorial plane and trans to a bridging oxygen of the V_2O_2 core are referred to here as G rings. The alcoxy units form a second type of pseudoequatorial ring referred to here as A rings. The theoretical angle sum of an A ring will be the same as the E ring (527.9°).

Results for the sum of the five-member ring angles are given in Table IV for $Co(edta)^-$, $[Cr(edda)(OH)]_2$, and $[V(hedta\text{-}H)]_2^{2-}$. The R rings containing $O_{3,1}$–V_1 and $O_{7,2}$–V_2 coordination in $[V(hedta\text{-}H)]_2^{2-}$ are of comparable strain to the R rings of $Co(edta)^-$ and $[Cr(edda)(OH)]_2$. These R rings are at longer hydrogen-bonded distances from the ethylenediammonium cation than the second set of R rings having carboxyl oxygen atoms $O_{6,1}$ and $O_{6,2}$ (see Table IIc) which are more strongly hydrogen bonded to the enH_2^{2+} cation. This second R ring set (average sum = 526.7°) is more strained by 11.1° than the R rings of $Co(edta)^-$. The structure of $Ca[Ca(edta)]\cdot 7H_2O$ was recently completed, showing the central Ca^{2+} unit to have eight-coordination.[17] The root-mean-square average of the angle sum of the glycinate rings is 528.6°.[17] Therefore in higher coordination numbers the angle sum of the five-member rings is often comparable to the strain found in the R ring set containing $O_{4,1}$–V_1 and $O_{4,2}$–V_2 bonds of $[V(hedta\text{-}H)]_2^{2-}$. The strain of the E rings for V_1 and V_2 centers averages 518.5°. This is the same value as determined for the

Table IV. Bond Angle Sums in $Co(edta)^-$, $[Cr(edda)(OH)]_2$, and $[V(hedta\text{-}H)]_2^{2-}$

ring	ideal sum	Co-(edta)$^-$	[Cr(edda)-(OH)]$_2$	$[V(hedta\text{-}H)]_2^{2-}$ V_1	$[V(hedta\text{-}H)]_2^{2-}$ V_2
R	538.4	537.8	537.0	537.9	532.0
			534.0	525.6	527.8
E	527.9	520.9	518.6	519.2	517.7
G	538.4	523.5		520.3	516.3
A	527.9			519.1	518.2
ref	10	13	10	this work	

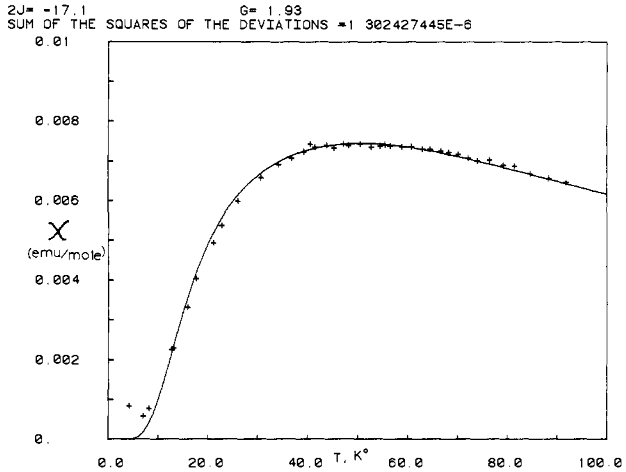

Figure 5. Temperature dependence of the magnetic susceptibilities of $[enH_2][V(hedta\text{-}H)]_2\cdot 2H_2O$.

---

(17) Barnett, R. L.; Uchtman, V. A. *Inorg. Chem.* **1979**, *18*, 2674.

(18) (a) Lewis, J.; Mabbs, R. E.; Richard, A. *Nature (London)* **1965**, *207*, 855. (b) Lewis, J.; Mabbs, R. E.; Richard, A. *J. Chem. Soc.* **1967**, 1014. (c) Reiff, W. M.; Baker, W. A.; Erichson, N. E. *J. Am. Chem. Soc.* **1968**, *90*, 4794.

(19) (a) Khedekar, A. V.; Lewis, J.; Mabbs, R. E.; Weigold, H.; *J. Chem. Soc.* **1961**, 1561. (b) Reiff, W. M.; Long, G. J.; Baker, *J. Am. Chem. Soc.* **1968**, *90*, 6347.

(20) (a) Schugar, H. J.; Walling, C.; Jones, R. B.; Gray, H. B. *J. Am. Chem. Soc.* **1967**, *89*, 3712. (b) Schugar, H. J.; Hubbard, A. P.; Anson, F. C.; Gray, H. B.; *Ibid.* **1969**, *91*, 71. (c) Schugar, H. J.; Rossman, G.; Barracough, C.; Gray, H. B. *Ibid.* **1972**, *94*, 2683.

(21) (a) Schugar, H. J.; Rossman, G.; Thibeault, J.; Gray, H. B. *Chem. Phys. Lett.* **1970**, *6*, 26. (b) Lohr, L. *Coord. Chem. Rev.* **1972**, *8*, 241. (c) Schugar, H. J.; Rossman, G.; Gray, H. B. *J. Am. Chem. Soc.* **1969**, *91*, 4564.

(22) Fleischer, E. B.; Palmer, J. M.; Srivastava, T. S.; Chatterjee, A. *J. Am. Chem. Soc.* **1974**, *93*, 3162.

(23) Thich, J. A.; Ou, C. C.; Powers, D.; Basilion, B.; Mastropaolo, D.; Potenza, J. A.; Schugar, H. J. *J. Am. Chem. Soc.* **1976**, *98*, 1425.

(24) Nortia, T.; Kontas, E. *Suom. Kemistil. B* **1971**, *44*, 406. Cf ref. 23.

(25) Kobayashi, H.; Haseda, T.; Kanda, E.; Mori, M. *J. Phys. Soc. Jpn.* **1960**, *15*, 1646.

(26) Earnshaw, A.; Lewis, J. *J. Chem. Soc.* **1961**, 396.

(27) Scaringe, R. P.; Singh, P.; Eckberg, R. P.; Hatfield, W. E.; Hodgson, D. J. *Inorg. Chem.* **1975**, *14*, 1127.

(28) Veal, J. T.; Hatfield, W. E.; Jeter, D. Y.; Hemgel, J. C.; Hodgson, D. J. *Inorg. Chem.* **1973**, 12, 342.

(29) Estes, E. D.; Scaringe, R. P.; Hatfield, W. E.; Hodgson, D. J. *Inorg. Chem.* **1976**, *15*, 1179.

(30) Veal, J. T.; Jeter, D. Y.; Hempel, J. C.; Eckberg, R. P.; Hatfield, W. E.; Hodgson, D. J. *Inorg. Chem.* **1973**, *12*, 2928.

(31) Shannon, R. D. *Acta Crystallogr. Sect. A* **1976**, *A32*, 751.

(32) Morrison, T. I.; Reis, A. H., Jr.; Knapp, G. S. Fradin, F. Y.; Chen, H.; Klippert, T. E. *J. Am. Chem. Soc.* **1978**, *100*, 3262.

(33) "International Tables of Crystallography"; Kynoch Press: Birmingham, England, 1900; Vol. III.

Table V. Antiferromagnetic Exchange for M(III) Binuclear Complexes

compd	μ_{eff}- (298 K)	$-2J$, cm^{-1}	ref
$[V(hedta\text{-}H)]_2^{2-}$	2.75	17.1	this work, 3
$[Fe(salen)]_2O$	1.87	190	18
$[Fe(o\text{-}phen)]_2O^{4+}$	1.74-1.83	190-120	19
$[Fe(hedta)]_2O^{2-}$	1.92	190	20c, 21c
$[Fe(TPP)]_2O$	1.86	200	22
$[Fe(Dipic)(H_2O)(OH)]_2$	4.86	22.8	23, 21c
$[Fe(chel)(H_2O)(OH)]_2$	5.24	14.6	23
$[Fe(H_2O)_4(OH)]_2^{4+}$		80	24, 25, 32
$[Cr(NH_3)_5]_2O^{4+}$		140	25, 26
$[Cr(o\text{-}phen)_2(OH)]_2^{4+}$		43.8	27
$[Cr(gly)_2(OH)]_2$		8.4	28
$[Cr(3Cl\text{-}acac)_2(OCH_3)]_2$		7.3	29
$[Cr(NH_3)_5]_2OH^{5+}$		32	30

$[Cr(edda)(OH)]_2$ complex and only 2.4° less than for the E ring of $Co(edta)^-$. The strain in the E rings of $[V(hedta\text{-}H)]_2^{2-}$ is then normal for complexes of edta-like ligands. The approximately equatorial G ring set of $[V(hedta\text{-}H)]_2^{2-}$ appears to be more strained than the G rings of $Co(edta)^-$ by an average of 5.2° in the angle sum. The A rings are observed to have angle sums very close to the experimental values for E rings of comparison complexes.

Magnetic Susceptibility of $[enH_2][V(hedta\text{-}H)]_2 \cdot 2H_2O$. The magnetic susceptibility data between 4.24 and 91.9 K are shown in Figure 5; the measured susceptibilities conform to the spin-only interaction of two d^2 ions with $S = 0$, 1, and 2 states as described by the Hamiltonian $-2J\mathbf{S}_1 \cdot \mathbf{S}_2$. A g value of 1.93 and a coupling constant of $2J = -17.1$ cm^{-1} are the best fit parameters required to provide the solid curve of Figure 5 as calculated from eq 3

$$\chi_M = \frac{Ng^2\beta^2}{kT} \frac{\sum(S^2 ... (-S)^2)e^{-S(S+1)J/kT}}{\sum(2S + 1)e^{-S(S+1)J/kT}} \tag{3}$$

throughout the temperature range. Therefore, the electronic spin moments of the two V(III) centers are only weakly antiferromagnetically coupled in contrast to the strong coupling observed for $(hedta)FeOFe(hedta)^{2-}$ complex of 1.92 μB for which the temperature dependence of the susceptibility suggests that $S_1 = S_2 = {}^5/_2$. A survey of transition-metal complexes which are known to be dihydroxy or dialcoxy bridged vs. those known to oxo bridged reveal $-2J$ values of about 20 cm^{-1} for alcoxy-bridged units and >140 cm^{-1} for oxo-bridged units. These comparisons are shown by Table V. The data for Fe(III) and Cr(III) complexes strongly support the dialcoxy structure for the $[V(hedta\text{-}H)]_2^{2-}$ complex ion.

Acknowledgement is made to the donors of the Petroleum Research Fund, administered by the American Chemical Society, for partial support of this work (grant for R.E.S.). We also acknowledge partial support of this work by the National Science Foundation through Grant No. CHE77-09913 for W.E.H.

Supplementary Material Available: Positional parameters for nonhydrogen atoms, fractional coordinates of atoms, and least-squares planes through atoms with deviations of atoms from planes are given in Tables SI, SII, and SIII (55 pages). Ordering information is given on any current masthead page.

Reaction of Carbon Monoxide with the Coordinately Unsaturated Metal Dimer $(\mu\text{-}H)_2Rh_2[P(O\text{-}i\text{-}C_3H_7)_3]_4$ with Retention of Dimeric Form. Crystal and Molecular Structure of $Rh_2(\mu\text{-}CO)_2[P(O\text{-}i\text{-}C_3H_7)_3]_4$

R. R. Burch,[1a] E. L. Muetterties,*[1a] A. J. Schultz,*[1b] E. G. Gebert,[1b] and Jack M. Williams*[1b]

Contribution from the Department of Chemistry, University of California, Berkeley, California 94720, and the Chemistry Division, Argonne National Laboratory, Argonne, Illinois 60439.

Received December 18, 1980. Revised Manuscript Received April 6, 1981

Abstract: The chemistry of $(\mu\text{-}H)_2Rh_2[P(O\text{-}i\text{-}C_3H_7)_3]_4$ with carbon monoxide is described. One equivalent of carbon monoxide irreversibly converted the dimer to $(\mu\text{-}H)_2Rh_2(\mu\text{-}CO)[P(O\text{-}i\text{-}C_3H_7)_3]_4$. The latter transformed slowly in solution to generate $Rh_2(\mu\text{-}CO)_2[P(O\text{-}i\text{-}C_3H_7)_3]_4$ and a second species presumed to be a hydride. The 30-electron $Rh_2(\mu\text{-}CO)_2[P(O\text{-}i\text{-}C_3H_7)_3]_4$ dimer reacted reversibly with carbon monoxide to give $Rh_2(\mu\text{-}CO)_2(CO)_2[P(O\text{-}i\text{-}C_3H_7)_3]_4$; no fragmentation to mononuclear metal complexes in this reaction system was observed up to 70 °C. Excess carbon monoxide did however elicit a fragmentation of the 30-electron complex, $(\mu\text{-}H)_2Rh_2(\mu\text{-}CO)[P(O\text{-}i\text{-}C_3H_7)_3]_4$. Reaction was rapid to give $HRh(CO)[P(O\text{-}i\text{-}C_3H_7)_3]_3$ and $HRh(CO)_2[P(O\text{-}i\text{-}C_3H_7)_3]_2$. The chemical and dynamic solution properties of these two mononuclear species is described; the properties of $HRh(CO)[P(O\text{-}i\text{-}C_3H_7)_3]_3$ diverge sharply from those of $HRh(CO)[P(C_6H_5)_3]_3$. From an X-ray diffraction study, the structure of $Rh_2(\mu\text{-}CO)_2[P(O\text{-}i\text{-}C_3H_7)_3]_4$ was established. In the $Rh_2(\mu\text{-}CO)_2$ framework, the rhodium atoms are separated by a distance of 2.630 (1) Å and the Rh_2C_2 array is not coplanar; rather the dihedral angle between the RhRh′C and RhRh′C′ planes is 140.8 (6)°.

Introduction

Polynuclear metal complexes present the possibility of defining in a formal context certain features of metal-surface chemistry. A constraint extant in the majority of known molecular metal clusters is their coordination saturation, a pervasive and significant feature that can substantially affect the nature of ligand bonding and result in reduced reactivity and enhanced potential for cluster fragmentation reactions. For these substantive issues, we have sought the synthesis of coordinately unsaturated metal clusters, compounds in which all or most of the metal atoms possess vacant coordination sites. Recently, we have described a series of co-

---

[1] (a) University of California, Berkeley, CA. (b) Argonne National Laboratory, Argonne, IL.

0002-7863/81/1503-5517$01.25/0 © 1981 American Chemical Society